

Optical Engineering

OpticalEngineering.SPIEDigitalLibrary.org

Microwave phase-control scheme based on optical beat wave generation and propagation in an optical fiber

Tomoyuki Uehara
Kenichiro Tsuji
Guido Mueller
David Tanner

SPIE.

Tomoyuki Uehara, Kenichiro Tsuji, Guido Mueller, David Tanner, "Microwave phase-control scheme based on optical beat wave generation and propagation in an optical fiber," *Opt. Eng.* **57**(1), 016106 (2018), doi: 10.1117/1.OE.57.1.016106.

Microwave phase-control scheme based on optical beat wave generation and propagation in an optical fiber

Tomoyuki Uehara,^{a,b,*} Kenichiro Tsuji,^a Guido Mueller,^b and David Tanner^b

^aNational Defense Academy of Japan, Department of Communications Engineering, Yokosuka, Kanagawa, Japan

^bUniversity of Florida, Department of Physics, Gainesville, Florida, United States

Abstract. A microwave phase-control scheme is proposed and experimentally demonstrated. Two lasers are combined in an optical fiber coupler to generate a beat signal. The beat frequency is tuned by controlling the frequency of one laser. Using the phase shift of the beat waves with different frequencies during the propagation in an optical fiber, the phase of the radio-frequency (RF) signal generated by a photodetector (PD) can be controlled. Using the phase shift during the propagation of beat waves in an optical fiber with different beat frequencies, the phase of the RF signal generated by a PD connected to the fiber can be controlled. A tunable phase shift ranging from 0 deg to 1400 deg is obtained for frequencies from 6 to 10 GHz. This scheme offers the advantages of fast tuning and precise phase control of an RF signal. © The Authors. Published by SPIE under a Creative Commons Attribution 3.0 Unported License. Distribution or reproduction of this work in whole or in part requires full attribution of the original publication, including its DOI. [DOI: [10.1117/1.OE.57.1.016106](https://doi.org/10.1117/1.OE.57.1.016106)]

Keywords: lasers; fibers; polarization-maintaining fiber; phase control.

Paper 171296 received Sep. 3, 2017; accepted for publication Dec. 15, 2017; published online Jan. 8, 2018.

1 Introduction

Radio-frequency (RF) phase shifters play an important role in phased-array antennas for radars (such as the phase shifters in the Aegis combat system)¹ and communication systems. Phased-array antennas usually employ conventional phase shifters based on ferrite materials,² PIN diodes,³ monolithic microwave integrated circuits,⁴ or liquid crystals.⁵ Electrical devices have narrow bandwidths and large losses compared with that in the photonic systems. The basic concepts behind photonic phase shifters for microwave signals have been reported.^{6,7} RF phase shifters based on photonic technology have a wide shift range. In the past decade, photonic RF phase shifters have been demonstrated using a nonlinear optical loop mirror⁸ and a single-sideband modulator.⁹ These require complex structures and specially designed devices. In contrast, simple techniques using optical fiber dispersion to implement a time delay have been developed, as summarized by Capmany et al.¹⁰ in a tutorial. In this paper, a microwave phase-control scheme based on beat note generation in an optical fiber without using dispersion is developed. The chromatic dispersion in our technique is not effective.¹¹ The phase of an RF signal converted from an optical beat by a photodetector (PD) can be shifted by a full 360 deg. The phase shift can be realized by controlling the detuning frequency of the beat note. The shift depends on the length of the optical fiber. Specifically, a longer fiber leads to a larger phase shift for the same beat note detuning. In this proposed scheme, the phase shift and signal frequency are related to each other. If a large frequency shift is desired, a long optical fiber should be used. Experimentally, the beat frequency is stabilized to the tunable output of a stable RF synthesizer^{12,13} to confirm the proposed concept.

The paper is structured as follows. First, we give a basic principle of RF phase shift and the frequency stabilization

technique of the beat note (Sec. 2). Then, we introduce the experimental setup (Sec. 3). In Sec. 3, we examine reasonable setup of the RF phase control using setup parameters. In Sec. 4, we consider the measured performance of the phase-controlled beat frequency signal. Finally, we give conclusions in Sec. 5.

2 Phase-Control Scheme

2.1 Basic Principle

The principle of the phase shift resulting from the beat frequency detuning is shown in Fig. 1. The phase-control system consists of two tunable lasers LD1 and LD2, a 3-dB fiber coupler, a fiber, and a PD. The outputs of the lasers are combined using the coupler and launched into the fibers where they create an optical beat note (interference pattern). The beat frequency of the initial state is

$$f_i = |f_1 - f_2|, \quad (1)$$

where f_1 and f_2 are the frequencies of the input lasers. The corresponding wavelength, or beat length, is

$$\lambda_i = \frac{c}{nf_i}, \quad (2)$$

where c and n are the speed of light in vacuum and the refractive index of the fiber, respectively. Thus, the initial phase ϕ_i in an optical fiber of length l is

$$\phi_i = \frac{nf_i l}{c} 360 \text{ deg}. \quad (3)$$

When f_2 is detuned to $f_2 + \Delta f$, the beat frequency becomes

$$f_c = |f_1 - f_2 - \Delta f| \quad (4)$$

*Address all correspondence to: Tomoyuki Uehara, E-mail: uehara@nda.ac.jp

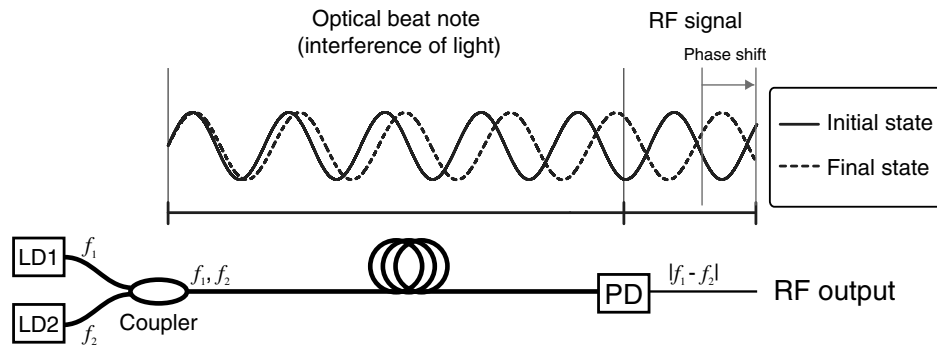


Fig. 1 Schematic of the phase-control system of the RF signal generated by optical beating. Here, LD denotes a laser diode and PD is a photodetector.

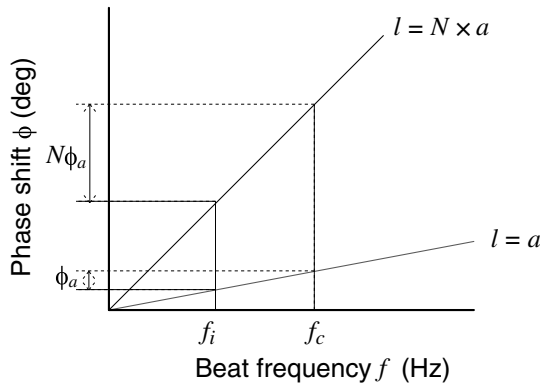


Fig. 2 Linear relationships between the phase shift ϕ , beat frequency f , and fiber length l .

and the corresponding phase becomes

$$\phi_c = \frac{nf_c l}{c} 360 \text{ deg.} \quad (5)$$

As a result, the phase shift of the beat note due to the frequency detuning Δf is

$$\Delta\phi = \phi_c - \phi_i = |\Delta f| \frac{nl}{c} 360 \text{ deg.} \quad (6)$$

By converting the beat note to an electrical signal using a PD, a phase-shifted RF output can be generated as shown in Fig. 1.

Figure 2 plots the theoretical relationship between the phase shift ϕ and the beat frequency f described by Eq. (6). The two lines show the phase shifts for fiber lengths of a and Na as linear functions of the detuning frequency Δf . When the fiber length is Na , the phase shift is $N\phi_a$, where ϕ_a is the phase shift for a fiber of length a .

The calculated RF phase shifts as a function of the detuning frequency and optical fiber length are graphed in Figs. 3 and 4, respectively. For a refractive index of 1.47, Eq. (6) predicts 1.76 deg/m/MHz. Therefore, detuning by 0.01 to 10 MHz results in phase shifts of 0.02 deg to 20 deg for a 1-m fiber. The phase shift can be extended to 200 deg by increasing the fiber length to 10 m. However, in a longer fiber, the phase shift is more sensitive to the detuning frequency, so the frequency stability of the beat note becomes a limiting factor. Here, the beat note frequency is stabilized to

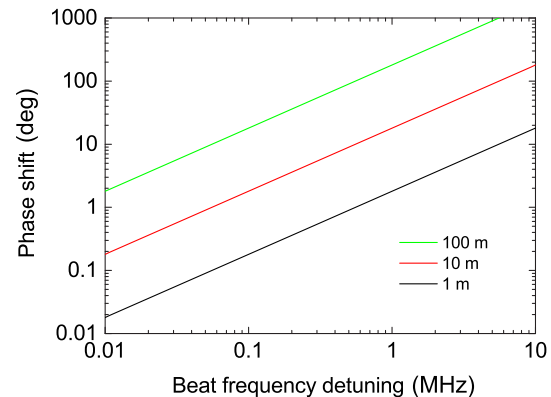


Fig. 3 Phase shift of an RF signal versus the detuning for fiber lengths of 1, 10, and 100 m.

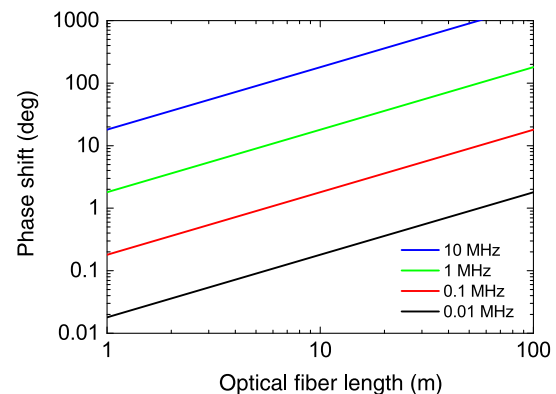


Fig. 4 Phase shift of an RF signal versus the fiber length for detuning frequencies of 0.01, 0.1, 1, and 10 MHz.

an external RF signal. The details of the stabilization method are described in Sec. 2.2.

Any desired phase shift can be obtained by a combination of fiber length and detuning frequency. Figure 5 considers combinations of these two parameters to obtain various phase shifts ranging from 0 deg to 180 deg.

On the other hand, Eq. (6) suggests that a large phase shift caused by a large frequency detuning results in a significant frequency change of the RF signal itself. This RF frequency shift may be undesirable for some applications. Dividing

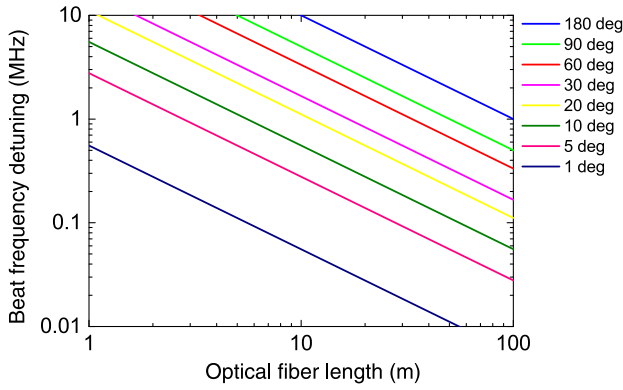


Fig. 5 Combinations of frequency detuning and fiber lengths to obtain specific phase shifts.

both sides of Eq. (6) by F , the frequency of the generated RF signal, results in

$$\frac{\Delta\phi_{\max}}{F} = \frac{|\Delta f_{\max}|}{F} \frac{nl}{c} 360 \text{ deg}, \quad (7)$$

where $\Delta\phi_{\max}$ and Δf_{\max} are the maximum phase shift and detuning frequency, respectively. Defining $|\Delta f_{\max}|/F$ to be the detuning ratio R_{detun} , Eq. (7) becomes

$$\Delta\phi_{\max} = R_{\text{detun}} \frac{nl}{c} 360 \text{ deg } F. \quad (8)$$

One can thereby calculate the maximum phase shift for a given RF signal frequency F and detuning frequency $|\Delta f_{\max}|$ as a function of the fiber length l . To keep the frequency change of the RF signal small, R_{detun} has to be kept small.

2.2 Frequency Stabilization of the Beat Note

A setup for beat frequency stabilization is shown in Fig. 6. It stabilizes the beat note generated by two lasers (LD1 and LD2) relative to a stable and tunable external RF signal. An RF self-heterodyne interferometer is introduced to generate the error signal proportional to the frequency difference. An error signal proportional to the frequency difference between the beat and RF synthesizer signals is converted to a DC signal applied to LD2 to control its frequency.

The RF signal intensity I generated by the PD is proportional to the intensity of the incident light

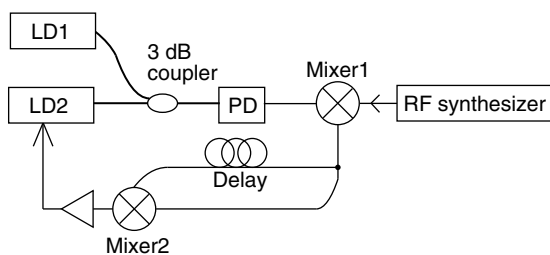


Fig. 6 Experimental setup for beat note stabilization. Here, LD is a laser diode and PD is a photodetector.

$$\begin{aligned} I &\propto \left| E_1 \cos(\omega_1 t) + E_2 \cos(\omega_2 t) \right|^2 \\ &= E_1^2 \cos^2(\omega_1 t) + E_2^2 \cos^2(\omega_2 t) + E_1 E_2 \cdot \cos[(\omega_1 + \omega_2) \cdot t] \\ &\quad + E_1 E_2 \cdot \cos[(\omega_1 - \omega_2) \cdot t], \end{aligned} \quad (9)$$

where E_1 and E_2 are the amplitudes of the electric fields of the optical beams of frequencies ω_1 and ω_2 , respectively.

Since the DC and higher frequency components are in the outside of the PD bandwidth, they are not detected. As a result, the low RF component [i.e., the last term in Eq. (9)] can be observed. To stabilize the beat note to a reference frequency of the synthesizer, the signal of frequency ω_{Synth} is multiplied by the beat signal using Mixer1, and the difference frequency component $\Delta\omega - \omega_{\text{Synth}}$, where $\Delta\omega = \omega_1 - \omega_2$ is downconverted to create an error signal for the stabilization. The component is then split into two equal parts, one of which is multiplied in Mixer2, while the other passes through a delay line. A coaxial cable is used to create a delay time τ between the two signals. That time τ is equivalent to a phase shift ϕ of $\tau(\Delta\omega - \omega_{\text{Synth}})$. As a result, the error signal from Mixer2 is

$$S \propto \cos \phi = \cos[\tau(\Delta\omega - \omega_{\text{Synth}})].$$

By scanning the frequency of LD1 or LD2 (i.e., by varying $\Delta\omega$), the error signal becomes a cosine curve of finite width corresponding to the bandwidth of Mixer2. That error signal has several zero-crossing points, one of which is used as a locking point.

3 Experiment

Figure 7 shows the experimental setup for a phase-control scheme using optical beat wave generation and propagation. Three RF signals are generated: an RF signal from PD1 used for the frequency control, a phase-shifted RF signal from PD2, and a reference signal from PD3.

An external-cavity diode laser (ECL) and a distributed-feedback (DFB) laser are used as optical sources to generate a beat signal. Since the frequency of the ECL can be tuned over a wide range, it is used for coarse tuning of the beat frequency. The DFB laser and servo system are used for fine-tuning of the beat frequency via the injection current. The optical output signals from the ECL and DFB laser are combined using a 2×2 3-dB polarization-maintaining (PM) fiber coupler in its orthogonal polarization state. The optical beat used for the frequency-control system is detected by fast photodiode PD1 and converted to an RF signal. The converted signal is boosted by RF amplifiers into the range from -10 to $+4$ dBm and used for frequency stabilization of the beat note. The details of the frequency stabilization method are described in Ref. 13. The beat frequency is approximately equal to the sum of the RF synthesizer frequency and an 8-MHz offset frequency. To investigate the dependence of the phase shift on the fiber length, extension fibers (measuring ~ 2 or 4 m) are inserted between the upper output fiber from the second 3-dB coupler and the polarizer. Even without an extension fiber, the path length from the 3-dB coupler to PD2 is longer than that from the coupler to PD3. This difference is an offset length in the setup. Thus, the optical path difference between the upper and lower paths is the length of the extension fiber plus the offset length.

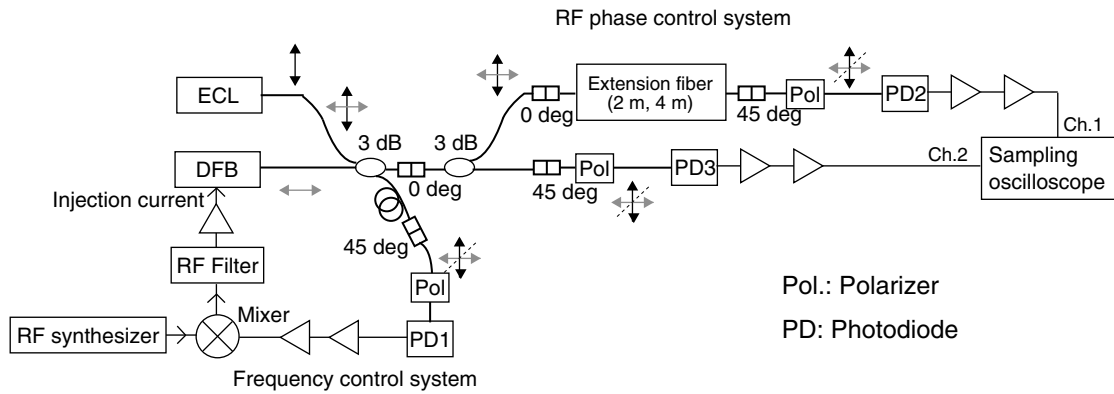


Fig. 7 Experimental setup for a phase-control scheme using optical beat wave generation and propagation. The beat frequency is locked to a stable and tunable RF external source. The lower path to the right of the second 3-dB coupler is used to generate a reference microwave signal. “0 deg” and “45 deg” indicate the connection angle of the PM optical fibers. For ease of adjustment of interference conditions between two laser lights, orthogonal polarization was used in this study.

The optical beat signal delayed by the extension fiber is converted into an RF signal by PD2. This becomes a phase-shifted RF signal on channel 1 of a sampling oscilloscope. The other signal from the second 3-dB coupler is converted into an RF signal by PD3 and boosted by two RF amplifiers to serve as a reference signal. The reference signal is measured on channel 2 and compared with the phase-shifted RF signal on channel 1.

4 Results

Measurements are performed at beat frequencies of ~6, 7, 8, 9, and 10 GHz. Since the beat frequency is locked to the external RF synthesizer frequency, the two frequencies differ only by the ~8-MHz offset from the feedback system.

The waveforms of the phase-shifted (channel 1) and reference (channel 2) RF signals measured by the sampling oscilloscope are shown in Fig. 8. No extension fiber is used

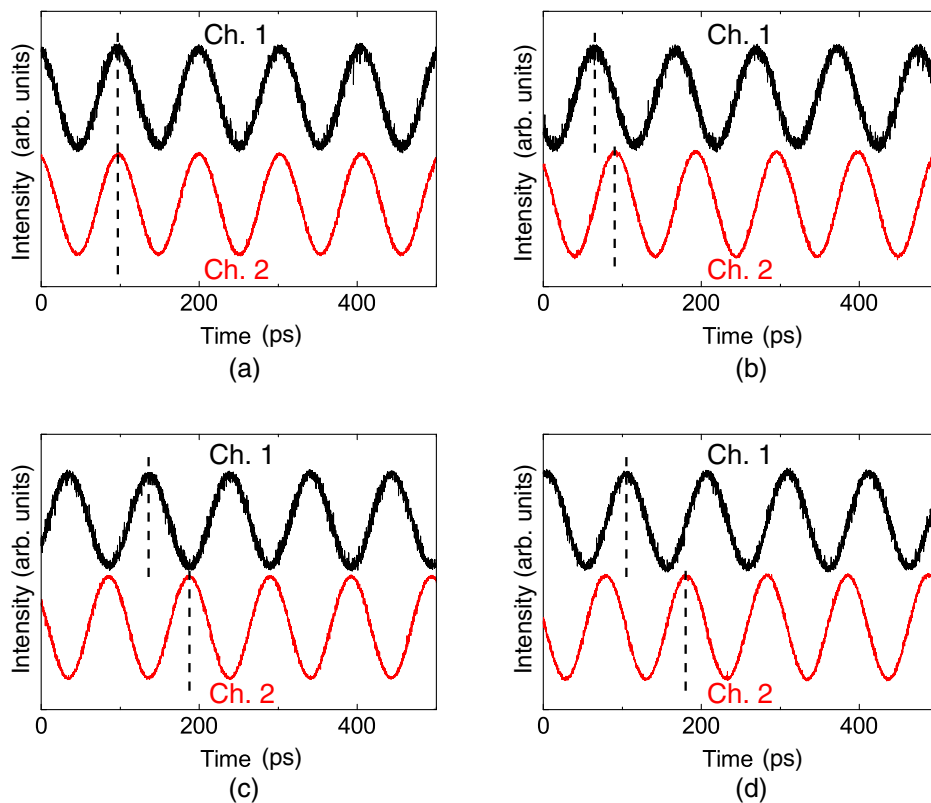


Fig. 8 Phase-shifted RF signal (Ch. 1) and reference RF signal (Ch. 2) measured by the sampling oscilloscope. By varying the frequency of the RF synthesizer, the phase difference of the beat note is shifted by (a) 0 deg (RF: 9.894 GHz), (b) 90 deg (RF: 9.908 GHz), (c) 180 deg (RF: 9.921 GHz), and (d) 270 deg (RF: 9.934 GHz). RF noise characteristics in each RF amplifier are not the same in each channel, so the signal in each channel has different noise characteristics.

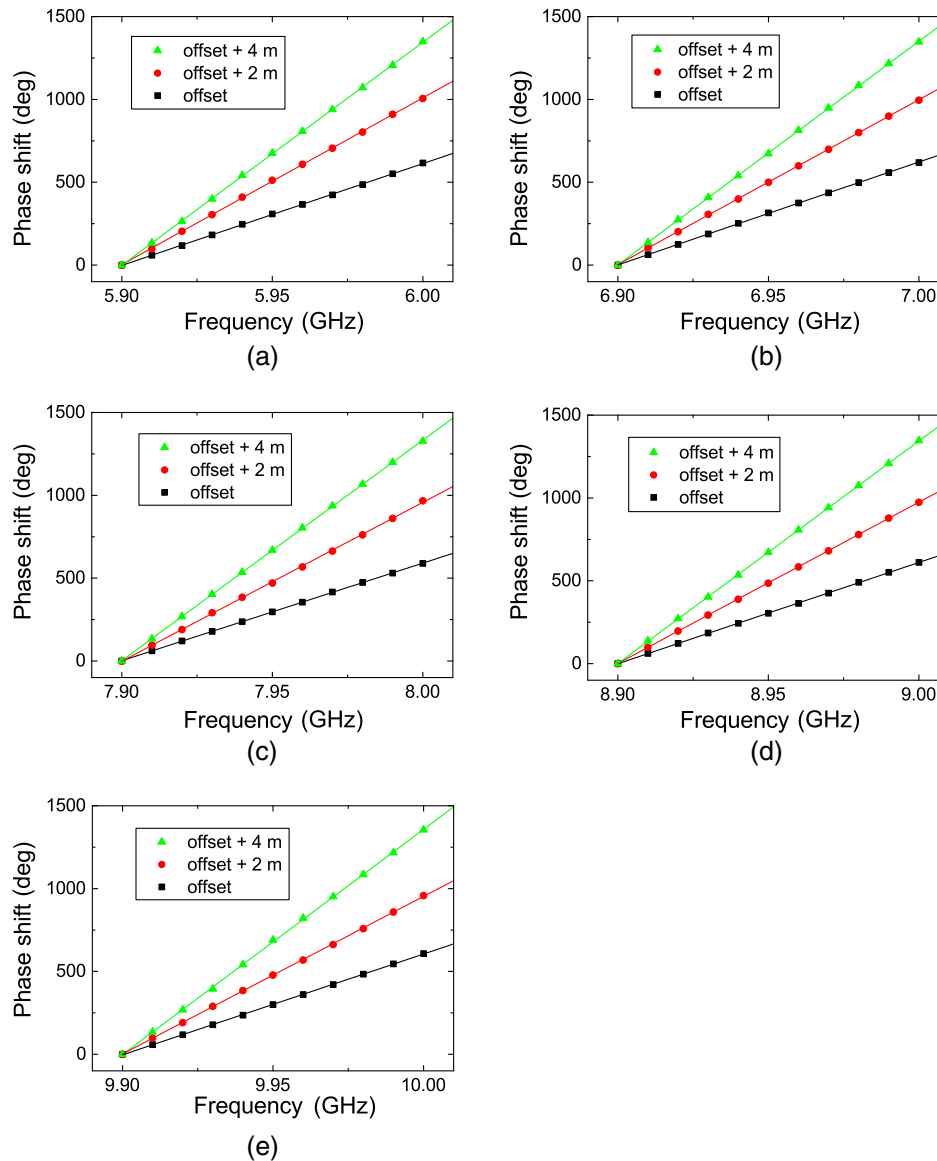


Fig. 9 Phase shift of the beat notes versus the RF synthesizer frequency for path lengths equal to the offset length, offset length + 2 m, and offset length + 4 m: (a) RF = 6 GHz, (b) RF = 7 GHz, (c) RF = 8 GHz, (d) RF = 9 GHz, and (e) RF = 10 GHz.

in this experiment. The frequency of the RF synthesizer is (a) 9.894, (b) 9.908, (c) 9.921, and (d) 9.934 GHz. The corresponding phase differences between the RF signals on channels 1 and 2 are 0 deg, 90 deg, 180 deg, and 270 deg, respectively. The phase-shifted signals (shown in black in Fig. 8) are noisy compared with the reference signals (shown in red in Fig. 8). This noise originates from the amplifiers used in the reference line. The frequencies of the RF signals generated by PD2 and PD3 are stable owing to the frequency stabilization system.

Figure 9 plots the phase difference between the RF signals on channels 1 and 2 for three different path lengths (namely, the offset only, offset + 2 m, and offset + 4 m) as a function of the RF synthesizer frequency near (a) 6, (b) 7, (c) 8, (d) 9, and (e) 10 GHz. As Eq. (6) indicates, the phase shift only depends on the frequency detuning and fiber length and not on the beat frequency. Based on these results, the rates of phase shift for the three different path lengths are found to be 6.758 deg/MHz for the offset only, 10.432 deg/MHz

for the offset + 2 m, and 14.125 deg/MHz for the offset + 4 m. The theoretical phase-shift factor is 1.76 deg/m/MHz according to Eq. (6). Dividing the phase-shift rate by this theoretical phase-shift factor, the calculated offset lengths between the upper and lower routes and the lengths of the two extension fibers are found to be 3.84, 2.09, and 4.18 m, respectively. These values are in good agreement with direct measurements.

4.1 Frequency Stability and Phase Fluctuation of the Generated RF Signal

The frequency stability (also called the square root of the Allan variance) of the RF signal is measured using a frequency counter. Our frequency-controlled system for the beat note between the two lasers has been optimized since the publication of Ref. 13. The frequency stabilization gain in low frequency in servo circuit was optimized by replacing one stage proportional–integral (PI) circuit to two stages PI,

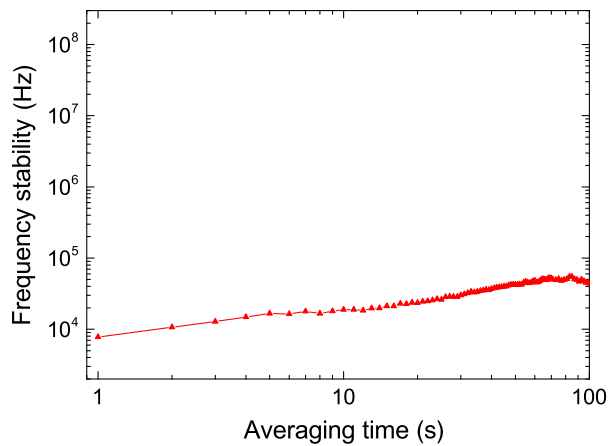


Fig. 10 Frequency stability of the beat note at 10 GHz.

so the frequency locking improved. The frequency stability of the system has improved from 400 kHz to lower than 10 kHz for an averaging time of 1 s. Figure 10 shows the measured fluctuations of the 10-GHz beat frequency, which are <50 kHz for an averaging time of 100 s.

The phase fluctuations in the generated RF signal are estimated from the residual between the experimental data and the linear fits in Fig. 9. For a beat frequency of 10 GHz, the standard deviation of the phase is 0.6 deg, 1.0 deg, and 2.0 deg for the offset only, offset + 2 m, and offset + 4 m, respectively. There are three possible origins of these fluctuations: RF signal fluctuations from the synthesizer, temperature variations, and vibration.

By assuming a 100-kHz frequency fluctuation of the RF signal, the phase fluctuations in the beat notes are estimated as $0.014 \text{ deg} = 360 \text{ deg} \times 100 \text{ kHz} / 10 \text{ GHz} \times 4 \text{ m}$, $0.022 \text{ deg} = 360 \text{ deg} \times 100 \text{ kHz} / 10 \text{ GHz} \times 6 \text{ m}$, and $0.029 \text{ deg} = 360 \text{ deg} \times 100 \text{ kHz} / 10 \text{ GHz} \times 8 \text{ m}$ for a fiber refractive index of 1.47.

The thermal expansion of the path length of an optical fiber is $9.39 \times 10^{-6} / ^\circ\text{C}$.¹⁴ The temperature of the laboratory is 20°C with a fluctuation of $\pm 1^\circ\text{C}$ during 10 min. Thus, the room temperature drift is estimated to be 0.2°C in the time needed to measure the phase shifts (i.e., in 1 min). For example, when the temperature changes from 20.0°C to 20.2°C , the length of a 4-m fiber changes by $7.51 \times 10^{-6} \text{ m} = 4 \text{ m} \times 9.39 \times 10^{-6} / ^\circ\text{C} \times 0.2^\circ\text{C}$. Dividing this value by one beat wavelength in the optical fiber (i.e., by 0.02 m assuming a refractive index of 1.47 and a 10-GHz beat frequency), the phase fluctuation is calculated to be 0.53 deg. Similarly, the phase fluctuations for a 6-m fiber (offset + 2-m fiber) and an 8-m fiber (offset + 4-m fiber) are found to be 1.19 deg and 2.12 deg, respectively.

Consequently, the net phase fluctuations are 0.53 deg, 1.19 deg, and 2.12 deg for the offset only, offset + 2-m fiber, and offset + 4-m fiber, respectively. These values are close to the standard deviations in our experimental environment. To achieve more accurate phase control, precise temperature control of the extension fiber and subkilohertz frequency stability of the control system are required.

5 Conclusion

A phase-shift scheme for RF signals generated by an optical beat method has been proposed and experimentally

demonstrated. The phase of an RF signal is tuned by controlling a beat frequency. Owing to the beat frequency stabilizer added to the phase-control system, stable phase control has been achieved. In the experiments, a tunable phase shift from 0 deg to 1400 deg was obtained over the frequency range from 6 to 10 GHz.

Acknowledgments

This work was supported by Japan Society for the Promotion of Science KAKENHI Grant No. 15K17479.

References

1. W. W. Bridger and M. D. Ruiz, "Total ownership cost reduction case study: AEGIS radar phase shifters," PhD Thesis, Naval Postgraduate School (2006).
2. G. M. Yang et al., "Novel compact and low-loss phase shifters with magnetodielectric disturber," *IEEE Microwave Wireless Compon. Lett.* **21**(5), 240–242 (2011).
3. S. Sengupta and K. U. Kiran, "Miniatured phase shifter," *Indian J. Sci. Technol.* **8**, 1–7 (2015).
4. C. Mengyi et al., "Ka-band full-360 analog phase shifter with low insertion loss," *J. Semicond.* **35**, 105005 (2014).
5. S. A. Attya et al., "Novel phase shifter based on dielectric resonator on liquid crystal substrate," *Appl. Comput. Electromagnet. Soc. J.* **30**, 365–373 (2015).
6. D. Novak and R. Waterhouse, "Advanced radio over fiber network technologies," *Opt. Express* **21**, 023001 (2013).
7. D. Jager, "Microwave photonics: from concepts to devices and applications," Chapter 1 in *Microwave Photonics*, 2nd ed., C. H. Lee, Ed., pp. 2–42, CRC Press (Taylor & Francis), New York (2013).
8. Y. Dong et al., "Photonic microwave phase shifter/modulator based on a nonlinear optical loop mirror incorporating a Mach Zehnder interferometer," *Opt. Lett.* **32**, 745–747 (2007).
9. W. Zhang and J. Yao, "Ultrawideband RF photonic phase shifter using two cascaded polarization modulators," *IEEE Photonics Technol. Lett.* **26**, 911–914 (2014).
10. J. Capmany, B. Ortega, and D. Pastor, "Free-space optical communications," *J. Lightwave Technol.* **24**, 201–229 (2006).
11. H. Schmuck, "Comparison of optical millimeter-wave system concepts with regard to chromatic dispersion," *Electron. Lett.* **31**(21), 1848–1849 (1995).
12. U. Schunemann and H. Engler, "Simple scheme for tunable frequency offset locking of two lasers," *Rev. Sci. Instrum.* **70**, 242–243 (1999).
13. T. Uehara et al., "Optical beat-note frequency stabilization between two lasers using a radio frequency interferometer in the gigahertz frequency band," *Opt. Eng.* **53**, 124109 (2014).
14. N. Sugimoto, "Temperature dependences of optical path length in inorganic glasses," *Res. Rep. Asahi Glass Co.* **57**, 75–81 (2007).

Tomoyuki Uehara is a junior associate professor/lecturer at the National Defense Academy of Japan and a visiting scholar at the University of Florida, USA. He withdrew from the doctoral program with the completion of course requirements from Kyoto University, Japan. He received his PhD in engineering by thesis in 2015. His current research interests include frequency stabilization of lasers (microwave photonics, gravitational waves, and axions).

Kenichiro Tsuji received his PhD in engineering from Niigata University, Niigata, Japan, in 1999. He joined the Department of Communications Engineering, National Defense Academy of Japan in 1999 and is currently an associate professor. His current research interests are photonic generation of coded RF signal and fiber-optic sensors based on Brillouin scattering.

Guido Mueller received his PhD in physics from the University of Hannover, Hannover, Germany, in 1998. He joined the Department of Physics, University of Florida, in 2003 and is currently a professor. His current research interests are axion-like particle search, LISA interferometry measurement system, gravitational reference sensor, advanced LIGO, and international REU for gravitation.

David Tanner received his PhD in physics from Cornell University, New York, USA, in 1972. He joined the Department of Physics, University of Florida, in 1982 and is currently a professor. His current research interests are condensed matter (optical properties of innovative materials) and astrophysics (axions and gravitational waves).